ELSEVIER

Physics Letters B 546 (2002) 55–62

PHYSICS LETTERS B

www.elsevier.com/locate/npe

Structure of ^{52,54}Ti and shell closures in neutron-rich nuclei above ^{48}Ca

R.V.F. Janssens [a,*], B. Fornal [b], P.F. Mantica [c,d], B.A. Brown [c,e], R. Broda [b], P. Bhattacharyya [f], M.P. Carpenter [a], M. Cinausero [g], P.J. Daly [f], A.D. Davies [c,e], T. Glasmacher [c,e], Z.W. Grabowski [f], D.E. Groh [c,d], M. Honma [h], F.G. Kondev [a], W. Królas [b], T. Lauritsen [a], S.N. Liddick [c,d], S. Lunardi [i], N. Marginean [g], T. Mizusaki [j], D.J. Morrissey [c,d], A.C. Morton [c], W.F. Mueller [c], T. Otsuka [k], T. Pawlat [b], D. Seweryniak [a], H. Schatz [c,e], A. Stolz [c,e], S.L. Tabor [l], C.A. Ur [i], G. Viesti [i], I. Wiedenhöver [a,l], J. Wrzesiński [b]

[a] *Argonne National Laboratory, Argonne, IL 60439, USA*
[b] *Niewodniczański Institute of Nuclear Physics, PL-31342 Cracow, Poland*
[c] *National Superconducting Cyclotron Laboratory, Michigan State University, East Lansing, MI 48824, USA*
[d] *Department of Chemistry, Michigan State University, East Lansing, MI 48824, USA*
[e] *Department of Physics and Astronomy, Michigan State University, East Lansing, MI 48824, USA*
[f] *Chemistry and Physics Departments, Purdue University, West Lafayette, IN 47907, USA*
[g] *INFN, Laboratori Nazionali di Legnaro, I-35020 Legnaro, Italy*
[h] *Center for Mathematical Sciences, University of Aizu, Tsuruga, Ikki-machi, Aizu-Wakamatsu, Fukushima 965-8580, Japan*
[i] *Dipartimento di Fisica dell'Università, and INFN Sezione di Padova, I-35131 Padova, Italy*
[j] *Institute of Natural Sciences, Senshu University, Higashimita, Tama, Kawasaki, Kanagawa 214-8580, Japan*
[k] *Department of Physics, University of Tokyo, Hongo, Tokyo 113-0033, Japan and RIKEN, Hirosawa, Wako-shi, Saitama 351-0198, Japan*
[l] *Department of Physics, Florida State University, Tallahassee, FL 32306, USA*

Received 11 July 2002; received in revised form 27 August 2002; accepted 9 September 2002

Editor: V. Metag

Abstract

The level structure of $^{54}_{22}\mathrm{Ti}_{32}$ has been explored for the first time by combining β-decay measurements from fragmentation products with prompt γ-ray spectroscopy following deep inelastic reactions. The latter technique was also instrumental in tracing $^{52}\mathrm{Ti}_{30}$ to higher spin. The data provide new tests of effective interactions for full pf-shell calculations in neutron-rich nuclei above ^{48}Ca. The data indicate the presence of a significant subshell gap at $N = 32$ and comparisons between theory and experiment suggest an additional shell closure at $N = 34$ in Ca and Ti isotopes.

* Corresponding author.
E-mail address: janssens@anl.gov (R.V.F. Janssens).

0370-2693/02/$ – see front matter
PII: S0370-2693(02)02682-5

The structure of neutron-rich nuclei has recently become the focus of much theoretical and experimental effort. Central to the on-going investigations is the expectation that substantial modifications can occur to the intrinsic shell structure of nuclei with a sizable neutron excess [1]. Alterations to the energy spacings of the orbitals and/or to their ordering can have a considerable impact on global nuclear properties such as the nuclear shape or the type of excitations characterizing the low-energy level spectra. The so-called "island of inversion" phenomenon discovered in neutron-rich exotic nuclei near $N = 20$ (^{30}Ne, ^{31}Na, $^{32–34}$Mg) [2] is perhaps one of the best examples so far of an unanticipated structural change. The "inversion", i.e., the presence of deformed rather than spherical ground-state configurations, results from promotions of neutrons across the $N = 20$ shell closure and has been attributed to strong interactions between valence protons and the promoted neutrons, interactions between the promoted neutrons themselves, and shifts in single particle energies [3].

Interactions between protons and neutrons have also been invoked to account for the presence of a subshell gap at $N = 32$ in neutron-rich nuclei located in the vicinity of the doubly-magic nucleus $^{48}_{20}$Ca$_{28}$ [4]. Specifically, it has been proposed that a weakening of the $\pi 1f_{7/2}$–$\nu 1f_{5/2}$ proton–neutron monopole interaction as protons are removed from the $1f_{7/2}$ single-particle orbital (filled at $Z = 28$), combined with a significant $2p_{1/2} - 2p_{3/2}$ spin-orbit splitting results in the emergence of the $N = 32$ subshell in nuclei such as $^{52}_{20}$Ca and $^{56}_{24}$Cr [4]. This subshell manifests itself by the large excitation energy of the first 2^+ state. More recently, shell-model calculations introducing a new effective interaction for pf-shell nuclei have been carried out [5]. They are able to account for the observations of Ref. [4]. In particular, the energy of the first 2^+ states in Ca, Ti, Cr, Fe and Ni isotopes are well reproduced. Interestingly, these calculations also suggest the presence of an additional $N = 34$ shell gap in the Ca and Ti isotopic chains. Note that the importance of the $V_{\sigma\tau}$ contribution to the $\pi 1f_{7/2}$–$\nu 1f_{5/2}$ proton–neutron monopole interaction and its role in forming the $N = 34$ shell gap was originally pointed out in Ref. [6].

The purpose of this Letter is two fold. First, the observation that the $N = 32$ subshell gap survives in the presence of $f_{7/2}$ protons, which so far relies mostly on the Cr systematics of Ref. [4], is reinforced by presenting first data on the $^{54}_{22}$Ti nucleus. Second, new tests of the effective interaction for pf-shell nuclei [5] are carried out by confronting the level structures of ^{52}Ti and ^{54}Ti up to medium spin ($I \geqslant 10$) with the results of shell-model calculations. These new data have been obtained by combining two experimental techniques seldom used together to investigate exotic nuclei: β-decay studies of products from a fragmentation reaction and in-beam γ-ray spectroscopy following deep-inelastic reactions. This approach was necessary because the two Ti isotopes of interest are neutron-rich and cannot be readily investigated at high spin with the more commonly used (HI,xn) fusion-evaporation reactions.

Prior to the present studies, nothing was known about the excited states of ^{54}Ti. Information about low lying levels was obtained from an investigation of the β decay of the parent, ^{54}Sc, produced with the experimental facilities at the National Superconducting Cyclotron Laboratory (NSCL). A primary beam of ^{86}Kr was accelerated to 140 MeV/nucleon with the new Coupled Cyclotron Facility, and fragmented on a 376 mg/cm^2 ^{9}Be target placed at the object position of the A1900 fragment separator [7]. A 330 mg/cm^2 Al degrader was located at the intermediate image of the A1900 separator to select fragmentation products with a given mass-to-charge ratio. A cocktail beam containing ^{54}Sc (1%), ^{55}Ti (14%), ^{56}V (24%), ^{57}V (26%), and ^{58}Cr (34%) was delivered to the NSCL β counting system. Fragment identification was derived in part from the energy loss and time-of-flight information (with respect to the cyclotron frequency) provided by a 500 μm-thick Si PIN detector placed approximately one meter upstream from the counting system. The fragments were stopped in a 985 μm thick double-sided Si strip detector (DSSD) segmented into 40 1-mm strips in both the x and y dimensions. Details on the performance of the DSSD when used to correlate fragment implants with subsequent β decays are given in Ref. [8]. The DSSD was surrounded by two 500 μm thick Si PIN detectors serving as second energy loss detectors for β particles. The PIN-DSSD-PIN detector sandwich was backed by a 300 μm thick Si PIN particle veto detector. The focusing conditions were such that more than two-thirds of the active DSSD area was illuminated by the fragments and the average implantation rate was 200 Hz. A γ-ray de-

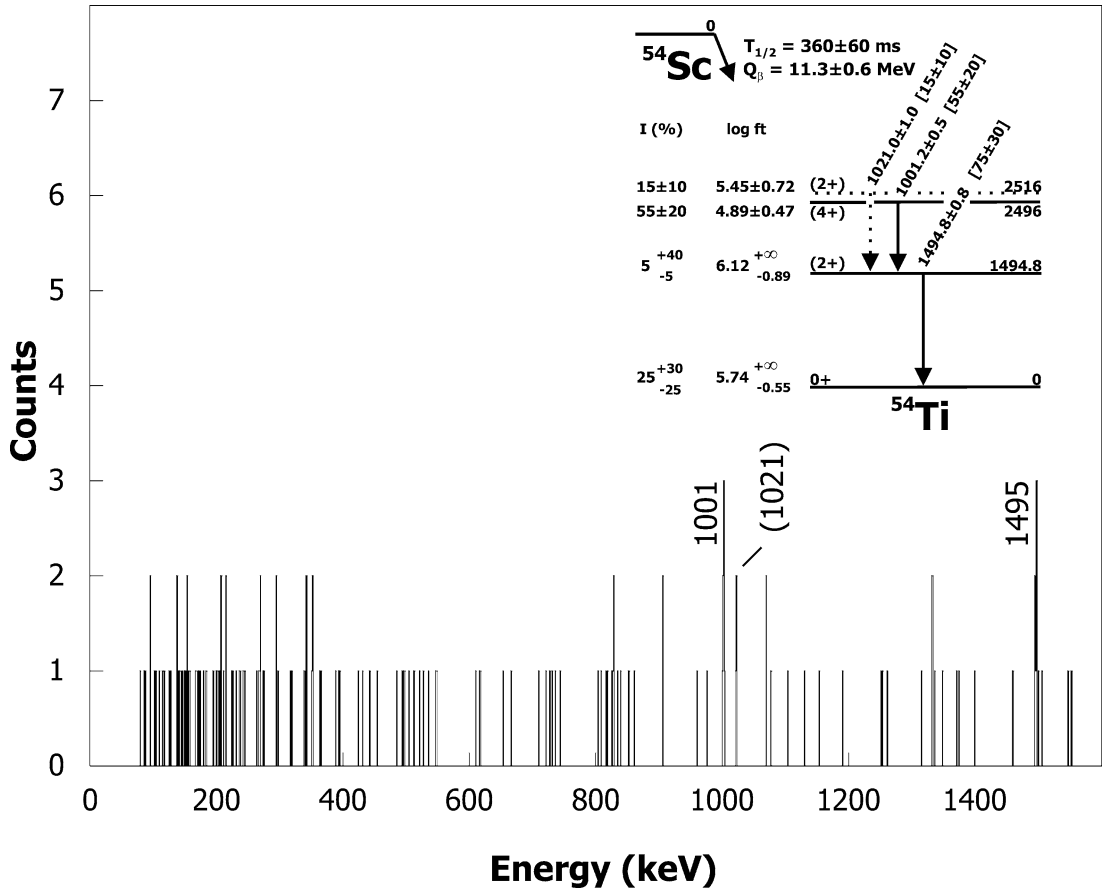

Fig. 1. Gamma-ray spectrum measured following the β decay of ^{54}Sc. The proposed level scheme and the associated decay characteristics (measured γ-ray intensities, deduced log ft values, etc.) are given in the insert.

tection efficiency of $\sim 3.3\%$ was achieved by placing six Ge detectors from the MSU Segmented Ge Array (SeGA) [9] in a circular geometry around the DSSD, with the long sides of the Ge cryostats parallel to the beam axis. An additional large volume Ge detector was positioned immediately behind the PIN-DSSD-PIN sandwich. Data were written event-by-event to disk every time any of the 80 strips of the DSSD fired. Each recorded event was tagged with an absolute time stamp generated by a free-running clock producing a pulse every 30.5 μs. Further experimental details can be found in Refs. [4,10].

In the analysis, fragment–β coincidences were established in software based on the correlation of valid implant and decay events following the procedures outlined in Refs. [4,8]. Briefly, an implant (decay) event was defined as one where a front and back strip of the DSSD fire in coincidence (in anti-coincidence) with the upstream Si PIN (energy-loss, time-of-flight) detector. Subsequent steps in the analysis consisted in correlating the fragment implant information (A, Z and time of implant) with the relevant β-decay data (decay curve and delayed γ-ray spectra). In order to reduce random fragment–β correlations a maximum time interval of ten seconds between any fragment-β correlation was imposed in software. A minimum time span of ten seconds between consecutive implants within a given pixel was required for the same reason. The measured efficiency for correlated β decays with ^{54}Sc implants was $\sim$30%.

The β-delayed γ-ray spectrum extracted for ^{54}Sc is presented in Fig. 1. This spectrum is a sum of all γ events observed within the first one second of a ^{54}Sc implant. Three weak transitions are observed

at 1001, 1021, and 1495 keV: they are attributed to the decay of excited levels in the daughter ^{54}Ti. The resulting low-energy level scheme is given as an inset in Fig. 1. The 1495 keV transition has the largest intensity and is proposed to correspond to the $2_1^+ \rightarrow 0_1^+$ transition. The absolute intensities of the 1495 and 1001 keV transitions suggest that they could be in cascade. However, the statistics in the $\gamma\gamma$ coincidence matrix was not sufficient to either support or refute this assertion. The log ft values were deduced from the absolute γ-ray intensity into and out of each proposed level. The β-decay Q value (Fig. 1) was derived from the measured mass excess for both parent and daughter as compiled in Ref. [11]. The half-life was deduced from a two-component fit to the decay curve correlated with ^{54}Sc implants, considering the parent decay and daughter growth and decay. The value $T_{1/2}^{\beta} = 360 \pm 60$ ms is somewhat larger than that reported previously by Sorlin et al., $T_{1/2}^{\beta} = 225 \pm 40$ ms [12]. This observation as well as other aspects of the β-decays of ^{54}Sc and other isotopes studied in the experiment are beyond the scope of the present work and will be discussed elsewhere [10].

A second, complementary experiment was carried out at the ATLAS accelerator at Argonne National Laboratory with the 101 Compton-suppressed Ge detectors of the Gammasphere multi-detector array [13]. A 305 MeV ^{48}Ca beam was sent on a 50 mg/cm^2 ^{208}Pb target. Data were collected when three or more Compton-suppressed Ge detectors fired in prompt coincidence. A total of 8.1×10^8 three and higher fold coincidence events were recorded on tape. The beam had an intrinsic time width of ~ 0.3 ns and was pulsed with a 400 ns repetition rate. This mode of operation provided a clean separation between prompt and isomeric events, and simplified both the observation of $\gamma\gamma$ correlations across isomers and the appropriate subtraction of random coincidence events. In the analysis, various conditions were placed on the time parameters to obtain prompt-prompt and prompt-delayed $\gamma\gamma$ matrices as well as the prompt $\gamma\gamma\gamma$ and prompt $\gamma\gamma$-delayed γ cubes.

Since nearly a decade, deep-inelastic reactions have been used successfully for structure investigations of neutron-rich nuclei [14]. The resolving power of the large detector arrays has proven sufficient to extract detailed information from coincidence data sets with large statistics, even for weak reaction channels. One difficulty in such studies is the assignment of an unknown sequence of γ rays to a specific product. The identification has often proven possible by using a cross coincidence technique with transitions in reaction partners [14]. In the present work, Hg nuclei are the complementary products in binary reactions leading to Ti isotopes, but a specific Ti isotope is in coincidence with several Hg partners because of neutron evaporation from the fragments after the collision. Unfortunately, the mass distribution of complementary fragments becomes particularly broad when product nuclei with large mass transfers are selected. Consequently, the identification of neutron-rich products is more difficult and sometimes ambiguous.

Spectra gated on yrast transitions in $A = 196$–204 Hg nuclei [15] provided strong coincidence relationships with known γ rays in the $A \leqslant 52$ Ti partners [15] and revealed new lines that could be tentatively associated with ^{53,54}Ti. The process is illustrated in Fig. 2(a), where the spectrum arising from a sum of double coincidence gates on known transitions in ^{196}Hg [16] is presented. As expected, this spectrum displays known lines from $^{50–52}$Ti [15] which are complementary to ^{196}Hg and are associated with 10, 9 and 8 evaporated neutrons, respectively. The complete analysis of cross-coincidence yields, which will be presented in a forthcoming paper on the ^{51}Ti and ^{53}Ti isotopes [17], assigned the 1237 and 1576 keV γ rays to ^{53}Ti (Fig. 2(a)). The cross correlation for the 1495 keV was, however, inconclusive. Hence, the β-decay measurement described above was of crucial importance to validate the ^{54}Ti assignment.

A spectrum gated with the 1495 keV transition (Fig. 2(b)) shows two strong, mutually coincident, γ rays with energies of 439 and 1002 keV. When ordered according to observed intensities ($I_\gamma(1495) = 100(8)$, $I_\gamma(1002) = 77(10)$, $I_\gamma(439) = 63(8)$), combined with the non-observation of the 439 keV line in β decay, these transitions establish the lowest three yrast levels in ^{54}Ti at 1495, 2497 and 2936 keV (Fig. 3). Thus, the tentative placement of the 1002 keV transition from the β-decay analysis is confirmed. There is little doubt that the 2497 and 2937 keV states correspond to the lowest 4^+ and 6^+ excitations as their strong population in the reaction indicates their yrast character. In addition, the sequence of transition ener-

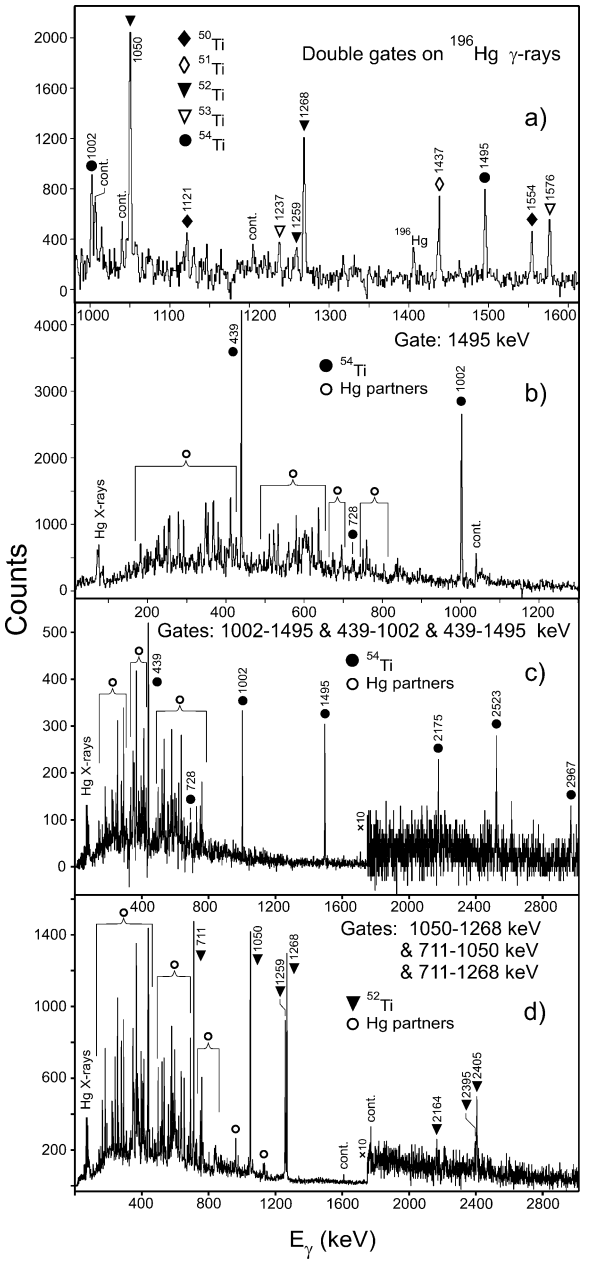

Fig. 2. Representative γ-ray spectra from the Gammasphere experiment; (a) high-energy part of a coincidence spectrum gated on yrast transitions in ^{196}Hg showing γ rays belonging to Ti partners, (b) spectrum from the prompt $\gamma\gamma$ coincidence matrix gated on the 1495 keV line (originally assigned to ^{54}Ti in the β-decay studies) showing clearly the next two transitions in the cascade as well as lines from the Hg reaction partners, (c) sum of double gates on selected ^{54}Ti γ rays used to find higher spin transitions in the nucleus, (d) same as (c), but for ^{52}Ti γ rays. See text for further details.

gies 439–1002–1495 keV is similar to the corresponding $6^+ \rightarrow 4^+ \rightarrow 2^+ \rightarrow 0^+$ cascade in ^{50}Ti with energies 524, 1121 and 1554 keV [15]. The inspection of double gates placed on the 1495, 1002, and 439 keV lines in the prompt $\gamma\gamma\gamma$ cube (see Fig. 2(c) for a representative example) revealed the presence of weaker 2175, 2523 and 2967 keV γ rays belonging to ^{54}Ti. Further analysis of spectra gated on these high-energy transitions identified additional coincident γ rays at 348, 728, 284, and 245 keV. The observed relationships and the measured intensities led to the level scheme given in Fig. 3 with additional states located at 5111, 5459, 5904, 6187, and 6432 keV. All spin assignments are tentative as no angular correlation information is available due to the weak intensity of this reaction channel. However, the fact that the reaction feeds yrast states preferentially, together with the close correspondence between established and calculated levels (see discussion below) allows one to assign spins with confidence along the sequence.

The construction of the ^{52}Ti level scheme was rather straightforward. Based on the available low lying levels [18], the coincidence spectrum of Fig. 2(d) was first obtained from the prompt $\gamma\gamma\gamma$ cube with gates placed on the 1050, 1268 and 711 keV lines corresponding to the known $2_1^+ \rightarrow 0_1^+$, $4_1^+ \rightarrow 2_1^+$ and $6_1^+ \rightarrow 4_1^+$ transitions. The strongest new γ rays appear clearly at 1259 and 2405 keV and establish new states at 4288 and 6693 keV. Further studies of the coincidence relationships with the latter lines provided evidence for the presence of an additional level at 9088 keV decaying through two parallel paths. As seen in Fig. 3, the strongest of these consists of a single, 2395 keV transition. In view of the weak intensities, the ordering in the parallel 231–2164 keV sequence is uncertain. As in ^{54}Ti, all spin and parity assignments above the 6^+ state are tentative, and rely on the assumption of preferential yrast feeding and on the close correspondence between established and calculated levels (see discussion below).

The first important result from the present measurements can be readily inferred from a close inspection of Fig. 3: the $E(2_1^+)$ energy dips from 1554 to 1050 keV between $^{50}Ti_{28}$ and $^{52}Ti_{30}$, before increasing significantly to 1495 keV in $^{54}Ti_{32}$. This behavior mirrors the one found by Prisciandaro et al. [4] in the Cr isotones ($E(2_1^+) = 1434$ (^{52}Cr), 835 (^{54}Cr)

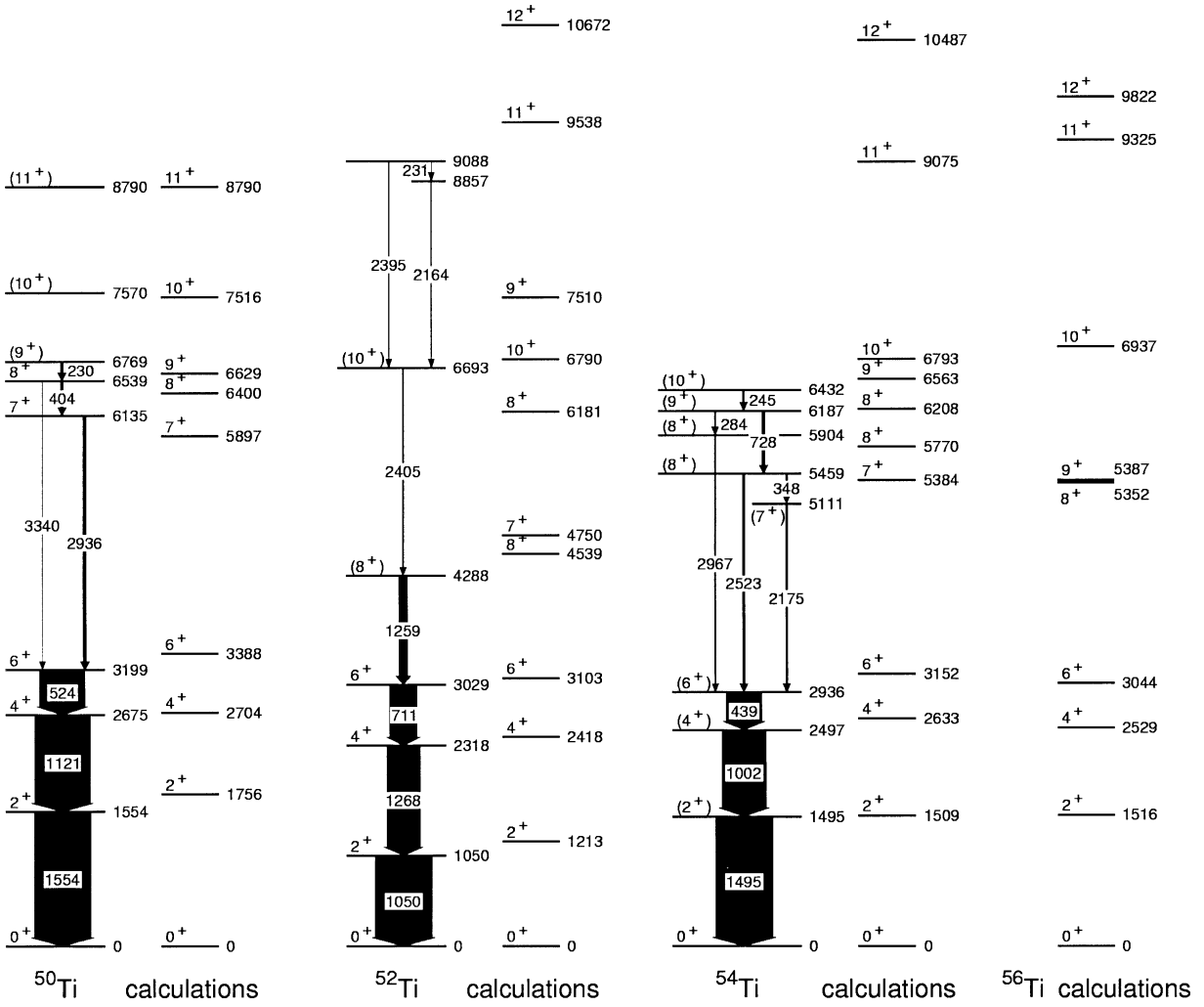

Fig. 3. Comparisons between shell-model calculations with the GXPF1 Hamiltonian and data for the even–even $^{50-54}$Ti isotopes. All the data for ^{54}Ti are from the present experiment as are those for $I \geqslant 8$ in ^{52}Ti. The width of the arrows is proportional to the measured intensities. The energy uncertainty for the strongest transitions in each nucleus is 0.2 keV, and increases to 0.6 keV for the weakest lines.

and 1007 keV (^{56}Cr). As pointed out in Ref. [4], this similarity also extends to the Ca isotones ($E(2_1^+) =$ 3832 (^{48}Ca), 1026 (^{50}Ca), and 2563 keV (^{52}Ca)), although the 2^+ assignment in ^{52}Ca is less certain. With the present data, an increase in the $E(2_1^+)$ excitation energy at $N = 32$ has now been confirmed for three isotopic chains, an observation consistent with the suggestion of a subshell closure at this neutron number. Another distinct feature of the level structures in Fig. 3 is the presence of higher-energy transitions ($E_\gamma \geqslant 2$ MeV) at moderate spins. Large jumps in transitions energies of this type are often regarded as signatures for excitations involving the breaking of the core, e.g., the valence space has been exhausted and higher angular momentum levels require excitations across a (sub)shell gap. In order to explore both of these observations further, a number of shell-model calculations were carried out.

The shell-model code MSHELL [19] was used to calculate the energies and wavefunctions of levels in the even–even $^{50-56}$Ti nuclei within the full pf-shell model space. The calculations were carried out with the five Hamiltonians FPD6 [20], KB3 [21], KB3G [22], GXFP1 and GXPF2 [5]. Many features

of the calculated yrast level schemes are similar with these five Hamiltonians. Hence, this Letter concentrates on comparisons between the data and calculations performed with the GXPF1 Hamiltonian, although significant differences with calculations carried out with the other interactions will be discussed as well. The GXFP1 Hamiltonian is of particular interest because it has recently been shown to be best in reproducing the $E(2_1^+)$ systematics for the Cr isotopes [23] where evidence for the $N = 32$ subshell closure was found.

The calculated GXPF1 energy levels are compared with the data in Fig. 3. The agreement with experiment is excellent and was used for spin-parity assignments. In particular, the change in the yrast pattern with neutron number is well reproduced and has a remarkably simple interpretation as the wavefunctions for most yrast levels are dominated (40–70%) by a single shell-model component. All of the isotopes start with a similar pattern in the energy spacing of the $J^\pi = 0^+, 2^+, 4^+, 6^+$ sequence which, according to the calculations, is due to the dominance of the $[\pi(f_{7/2})^2, J_p]$ proton configuration. This configuration is coupled to the following neutron configurations: $[\nu(f_{7/2})^8, J_n]$ in ^{50}Ti, $[\nu(f_{7/2})^8(p_{3/2})^2, J_n]$ in ^{52}Ti, $[\nu(f_{7/2})^8(p_{3/2})^4, J_n]$ in ^{54}Ti and $[\nu(f_{7/2})^8 (p_{3/2})^4(p_{1/2})^2, J_n]$ in ^{56}Ti. The latter are the same neutron configurations that dominate the ground states of ^{48,50,52,54}Ca, respectively. They are all closed-shell configurations (e.g., $J_n = 0$ only), except for the $\nu(p_{3/2})^2$ states in ^{52}Ti and ^{50}Ca where the $J_n = 0, 2$ couplings are relatively close in energy. As a consequence, the first 2^+ state in the Ca and Ti nuclei is relatively high, except in ^{50}Ca (see Fig. 1 in [5]). In the same way, mixing with the low-lying $J_n = 2$ neutron state is the reason that the $J^\pi = 0^+, 2^+, 4^+, 6^+$ spectrum of ^{52}Ti appears distorted compared to that of the other Ti isotopes. These features of the neutron configurations also explain the relatively low-lying 8^+ state in ^{52}Ti which originates from the $J_n = 2$ neutron configuration coupled to $J_p = 6$ protons. The fact that the neutron shell is closed also has important implications for the predicted structure of the more neutron-rich Ca and Ti nuclei that have not yet been reached experimentally. As predicted in Ref. [6] from a basic standpoint and shown in detail in calculations with the GXPF1 and GXPF2 interactions [5], ^{54}Ca will be a new closed-shell nucleus with a high $E(2_1^+)$ energy (~ 4 MeV, see Fig. 1 in Ref. [5]). This same property is reflected in the predicted location of the lowest ^{56}Ti 2^+ level as shown in Fig. 3.

The dominant component in the wavefunctions of the $J^\pi = 7^+, 8^+, 9^+, 10^+, 11^+$ levels in ^{50}Ti is $\{[\pi(f_{7/2})^2, J_p = 6], [\nu(f_{7/2})^7, J_n = 7/2], [\nu p_{3/2}, J_n' = 3/2]\}$. As can be seen in Fig. 3, the calculations reproduce the experimental spectrum (for comparison, spectra with the FPD6 and KB3G interactions are also available in Ref. [22]). In the heavier Ti isotopes, the levels associated with these $f_{7/2}$ neutron-hole configurations lie at higher excitation energy. For example, the 11^+ member of the $f_{7/2}$ neutron-hole state is at 9.54 MeV in ^{52}Ti (Fig. 3). The calculations indicate that the ^{52}Ti, 8_2^+ level is dominated by the configuration $[\nu(f_{7/2})^8(p_{3/2})(p_{1/2}), J_n = 2]$ coupled to the $[\pi(f_{7/2})^2, J_p = 6]$ protons, while the 10^+ state is based on the same protons coupled to $[\nu(f_{7/2})^8(p_{3/2})(f_{5/2}), J_n = 4]$ neutrons. In ^{54}Ti, the 7^+ and 8_1^+ states are dominated by the fully aligned $J_p = 6$ protons coupled $[\nu(f_{7/2})^8(p_{3/2})^3(p_{1/2}), J_n = 2]$, while the 9^+ and 10^+ levels correspond to the coupling with $[\nu(f_{7/2})^8(p_{3/2})^3(f_{5/2}), J_n = 3, 4]$ neutrons (the 8_2^+ state corresponds to a mixture of these two neutron configurations). Thus, the energies of these higher spin states depend upon the effective single-particle energies of the $p_{1/2}$ and $f_{5/2}$ orbitals, and the agreement with experiment provides a first crucial test of this part of the GXPF1 Hamiltonian which predicts the shell closure in ^{54}Ca.

The five Hamiltonians mentioned above differ mainly with regard to the location in energy of the $\nu f_{5/2}$ orbital in these neutron-rich nuclei. The KB3, GXPF1 and GXPF2 interactions are similar, with a relatively large $f_{5/2} - p_{3/2}$ effective single-particle gap near $Z = 20$ and $N = 34$. In contrast, the FPD6 and KB3G interactions are characterized by a smaller $f_{5/2} - p_{3/2}$ gap which lowers the calculated $J^\pi = 9^+$, 10^+ states in ^{54}Ti by about 0.8 MeV relative to GPX1 calculations, i.e., about 0.5 MeV too low compared to experiment. These FPD6 and KB3G Hamiltonians do not predict a shell closure in ^{54}Ca. It is clear that the ^{54}Ti data strongly support the calculations with a high $f_{5/2}$ effective single-particle energy at $N = 34$ and are, thus, pointing towards a shell closure in ^{54}Ca [6]. Furthermore, comparisons of a future experiment with the predicted spectrum of ^{56}Ti (Fig. 3) will provide ad-

ditional information regarding the magicity of ^{54}Ca. In particular, the large energy gap predicted between the 6^+ and 8^+ states in ^{56}Ti, and the high energy of the first 2^+ excited state are direct consequences of the doubly-closed shell nature of ^{54}Ca.

To summarize, by combining two experimental techniques, the level structure of ^{54}Ti was delineated for the first time. These data, together with new information gathered on ^{52}Ti, provide further evidence for a closed neutron subshell at $N = 32$ in neutron-rich nuclei above ^{48}Ca. More importantly, these results constitute important new tests of effective interactions for full pf-shell model calculations in this region of the nuclear chart. It was shown that the medium spin ($I \geqslant 8$) states test the Hamiltonians that have been proposed and support the view by some of these that an additional, new shell closure occurs at $N = 34$. These results also call for data on the first excited states of ^{56}Ti and ^{54}Ca to investigate this issue further. Experiments along these lines are underway.

Acknowledgements

This work was supported in part by the US Department of Energy, Nuclear Physics Division, under Contracts Nos. W31-109-ENG-38 and DE-FG02-87ER40346, by National Science Foundation Grant Nos. PHY-01-10253, PHY-00-70911 and PHY-97-24299, by Polish Scientific Committee Grant No. 2PO3B-074-18, and by Grant-in-Aid for Scientific Research No. (A)(2) (10304019) and by Grant-in-Aid for Specially Promoted Research (13002001) from the Ministry of Education, Science and Culture of Japan.

References

[1] B.A. Brown, Prog. Part. Nucl. Phys. 47 (2001) 517.
[2] See, for example, T. Motobayashi, et al., Phys. Lett. B 346 (1995) 9;
R. Ibbotson, et al., Phys. Rev. Lett. 80 (1998) 2081;
B.V. Prittychenko, et al., Phys. Rev. C 63 (2001) 011305(R), and references therein.
[3] E.K. Warburton, et al., Phys. Rev. C 41 (1990) 1147;
Y. Utsuno, et al., Phys. Rev. C 64 (2001) 011301.
[4] J.I. Prisciandaro, et al., Phys. Lett. B 510 (2001) 17.
[5] M. Honma, et al., Phys. Rev. C 65 (2002) 061301.
[6] T. Otsuka, et al., Phys. Rev. Lett. 87 (2001) 082502.
[7] D.J. Morrissey, Nucl. Instrum. Methods Phys. Res. B 126 (1997) 316;
D.J. Morrissey, et al., Nucl. Instrum. Methods Phys. Res. A, in press.
[8] J.I. Prisciandaro, A.C. Morton, and P.F. Mantica, Nucl. Instrum. Methods Phys. Res. A, in press.
[9] W.F. Mueller, et al., Nucl. Instrum. Methods Phys. Res. A 466 (2001) 492.
[10] P. Mantica, et al., in preparation.
[11] G. Audi, A.H. Wapstra, Nucl. Phys. A 595 (1995) 409.
[12] O. Sorlin, et al., Nucl. Phys. A 632 (1998) 205.
[13] R.V.F. Janssens, F.S. Stephens, Nucl. Phys. News 6 (1996) 9; I.Y. Lee, Nucl. Phys. A 520 (1990) 641c.
[14] R. Broda, Eur. Phys. J. A 13 (2002) 1, and references therein.
[15] R.B. Firestone, et al., Table of Isotopes, Vol. 1, Wiley.
[16] T.C. Zhou, et al., Nucl. Data Sheets 83 (1998) 145.
[17] B. Fornal, et al., in preparation.
[18] H. Junde, Nucl. Data Sheets 90 (2000) 1.
[19] T. Mizusaki, RIKEN Accel. Prog. Rep. 33 (2000) 14.
[20] W.A. Richter, et al., Nucl. Phys. A 523 (1991) 325.
[21] A. Poves, A.P. Zuker, Phys. Rep. 70 (1981) 235.
[22] A. Poves, et al., Nucl. Phys. A 694 (2001) 157.
[23] P.F. Mantica, et al., in preparation.